Available online at www.sciencedirect.com
ScienceDirect
Journal of Power Sources 178 (2008) 393–401
JOURNAL OF POWER SOURCES
www.elsevier.com/locate/jpowsour

Fe_2O_3-filled carbon nanotubes as a negative electrode for an Fe–air battery

Bui Thi Hang [a,*], Hiroshi Hayashi [b], Seong-Ho Yoon [c], Shigeto Okada [c], Jun-ichi Yamaki [c]

[a] *Japan Science and Technology Agency (JST), 6-1 Kasuga-koen, Fukuoka 816-8580, Japan*
[b] *Interdisciplinary Graduate School of Engineering Sciences, Kyushu University, 6-1 Kasuga-koen, Fukuoka 816-8580, Japan*
[c] *Institute for Materials Chemistry and Engineering, Kyushu University, 6-1 Kasuga-koen, Fukuoka 816-8580, Japan*

Received 6 November 2007; accepted 1 December 2007
Available online 15 December 2007

Abstract

Fe_2O_3-filled carbon nanotube material was prepared by filling carbon nanotubes (CNTs) with iron nitrate and then heating in an argon flow. The morphology and structure of this material were investigated by transmission electron microscopy (TEM), scanning electron microscopy (SEM) coupled with X-ray energy dispersive spectroscopy (EDS) and X-ray diffraction (XRD) measurements. The morphology, particle size and amount of iron oxide that filled CNTs depended on the amount of iron nitrate precursor. When Fe:C = 1:17 wt%, almost all of the iron oxide particles resided inside CNTs and their particle size was smaller than that at Fe:C = 1:8 wt%. The electrochemical properties of this material were investigated using cyclic voltammetry (CV) and galvanostatic cycling.
© 2008 Published by Elsevier B.V.

Keywords: Carbon nanotubes; Fe_2O_3-filled carbon nanotubes; Fe–air battery negative electrode

1. Introduction

Over the past several years, metal-filled carbon nanotubes or nanoparticles have attracted much attention due to their special electronic [1,2], magnetic [3–5] and optical [6] properties. These materials can be used for various important applications in nanotechnology [7–11], biomedical sciences [12,13] and memory device technology [13–18]. Moreover, they can also be used as electrode materials in electrochemical devices.

Several groups have reported the preparation of metal-filled carbon nanotubes [19–26] using different methods. In general, the methods for the synthesis of metal-filled carbon nanotubes can be classified into two main types: two-step and one-step. The former, such as a liquid chemical method, involves the opening of CNTs and filling them with liquid metal or metal salt solution [26]. In one-step methods, CNTs are prepared simultaneously with the addition of foreign substances or prepared in situ filled with metal by using a catalyst as the metal source [19–25]. However, the level of filling with these methods is often not satisfying. Moreover, for Fe- or Fe_2O_3-filled CNTs, in addition to the main product of iron or iron oxide, compounds of iron and carbon, such as Fe_3C, are also formed.

In our previous work [27], nano-sized Fe_2O_3-loaded carbon was prepared successfully and the effect of nano-size on the utilization of iron was investigated. Unfortunately, this material shows fading capacity with repeated cycling. This fading is mainly due to an increase in iron particle size and the dissipation of soluble $HFeO_2^-$ species in the electrolyte during cycling. Nano-sized Fe_2O_3 within carbon nanotubes is expected to show a limited particle size for iron and to inhibit the dissipation of soluble species upon cycling. Thus, in this study, we present a simple method for preparing Fe_2O_3-filled carbon nanotubes and also discuss their electrochemical properties.

2. Experimental

The carbon material used in this study was carbon nanotubes (CNTs) with an average diameter of ca. 50 nm. The CNTs were prepared as described previously [28]. Iron nitrate (Wako Pure Chemical Co.) was used as the iron source. CNTs were treated to remove catalyst before the preparation of Fe_2O_3-filled CNTs. Carbon material was immersed in chloride acid 10% and the mixture was agitated by a magnetic stirrer at room tem-

* Corresponding author. Tel.: +81 92 583 7790; fax: +81 92 583 7790.
E-mail address: HANG.Buithi@nims.go.jp (B.T. Hang).

0378-7753/$ – see front matter © 2008 Published by Elsevier B.V.
doi:10.1016/j.jpowsour.2007.12.012

perature for 3 days. CNTs were then removed, washed with ion-exchanged water and dried.

The Fe_2O_3-filled CNT material was prepared by dipping treated CNTs into an $Fe(NO_3)_3$ aqueous solution with an iron-to-carbon weight ratio of 1:17 or 1:8. The mixture was agitated by a magnetic stirrer over 4 days, dried at 50 °C, and then subjected to calcination for 1 h at 400 °C in flowing Ar. The iron compound obtained inside the nanotubes was identified to be Fe_2O_3 by X-ray diffraction. The actual weight of iron in the final Fe_2O_3-filled CNTs was checked by heating the as-prepared materials to 1000 °C under air to remove the carbon. The morphology of the as-prepared Fe_2O_3-filled CNT materials was observed by transmission electron microscopy (TEM) and scanning electron microscopy (SEM) together with X-ray energy dispersive spectroscopy (EDS).

To determine the electrochemical behavior of each Fe_2O_3-filled CNT material, an electrode sheet was prepared by mixing 90 wt% of the respective Fe_2O_3-filled CNTs and 10 wt% polytetrafluoroethylene (PTFE; Daikin Co.) and rolling. The Fe_2O_3-filled CNT electrode was made into a pellet 1 cm in diameter. Cyclic voltammetry studies were carried out with a three-electrode glass cell assembly that had the Fe_2O_3-filled CNT electrode as the working electrode, silver oxide as the counter electrode, Hg/HgO (1 M NaOH) as the reference electrode and cellophane, together with filter paper, as the separator, which was sandwiched between the two electrodes. The electrolyte used was 8 mol dm^{-3} aqueous KOH. Cyclic voltammetry measurements were recorded at a sweep rate of 0.1 mVs^{-1} and within a range of −1.2 V to −0.1 V. After 15 redox cycles, the Fe_2O_3-filled CNT electrodes were removed, washed with ion-exchanged water, dried and observed by SEM-EDS for comparison with the findings before cycling.

Galvanostatic cycling performance for the Fe_2O_3-filled CNT electrodes was measured with a three-electrode glass cell assembly. The discharge cutoff potential was −0.1 V, and a constant potential charging step was applied at −1.15 V after galvanostatic charging. A constant potential of −1.15 V was used because of the large amount of hydrogen evolution observed at around −1.2 V. The current densities for the charge and discharge processes were 0.5 mA cm^{-2} and 0.2 mA cm^{-2}, respectively.

3. Results and discussion

The X-ray patterns of the as-prepared materials with Fe:C = 1:17 wt% and 1:8 wt% are presented in Fig. 1. At different weight ratios of iron and carbon, an Fe_2O_3 phase is indeed present together with carbon in the product. This result suggested that the material contains Fe_2O_3 and carbon and the active material in this case is Fe_2O_3.

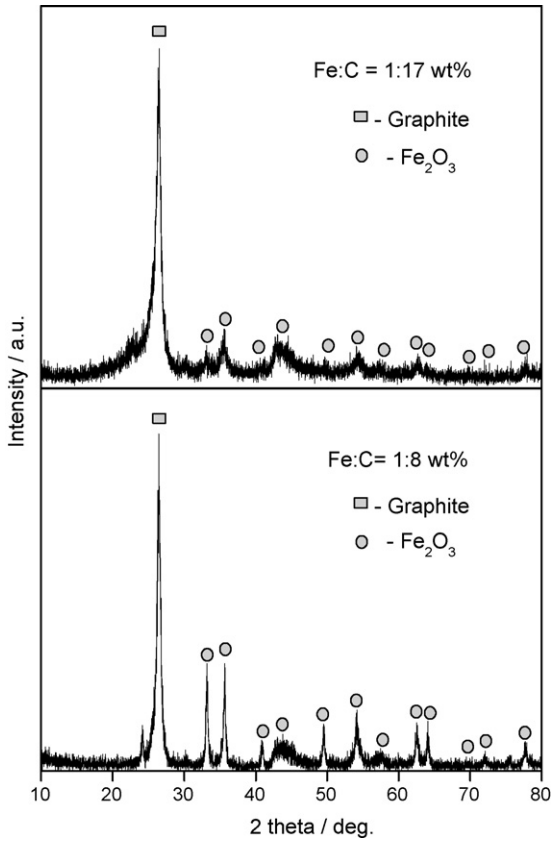

Fig. 1. X-ray pattern of as-prepared Fe_2O_3-filled CNTs with iron-to-carbon weight ratios of 1:17 and 1:8.

In these preparation conditions, the weight ratio of iron to carbon is 1:8 and 1:17. To determine the actual weight of iron oxide in the final Fe_2O_3-filled CNTs, the as-prepared materials were heated from room temperature to 1000 °C in air to remove the carbon. The amount of remaining material, which was considered to be Fe_2O_3, was compared with that under the preparation conditions. The results in Table 1 show that with both Fe:C = 1:17 wt% and 1:8 wt%, there was no significant difference between the amount of iron oxide in the obtained Fe_2O_3-filled CNTs and that in the preparation condition (Fe:C = 1:17.3 wt% and 1:8.2 wt%). There was very little difference between the amount of iron oxide in the preparation condition and that in the final material.

Fig. 2 shows TEM images of the as-prepared materials with Fe:C = 1:17 wt% and 1:8 wt% at various magnifications. The dark particles inside CNTs are Fe_2O_3. The TEM images show that the carbon nanotubes were filled with fine Fe_2O_3 particles. Various morphologies of Fe_2O_3 could be observed, such as particles and nanorods, which show very different sizes

Table 1
Results upon heating Fe_2O_3-filled CNTs at 1000 °C in air

Weight ratio in preparation condition (Fe:C)	Fe_2O_3 amount in preparation condition (mg)	Fe_2O_3 amount obtained from measurement (mg)	Weight ratio obtained from measurement (Fe:C)
1:17	3.72	3.66	1:17.3
1:8	7.33	7.22	1:8.12

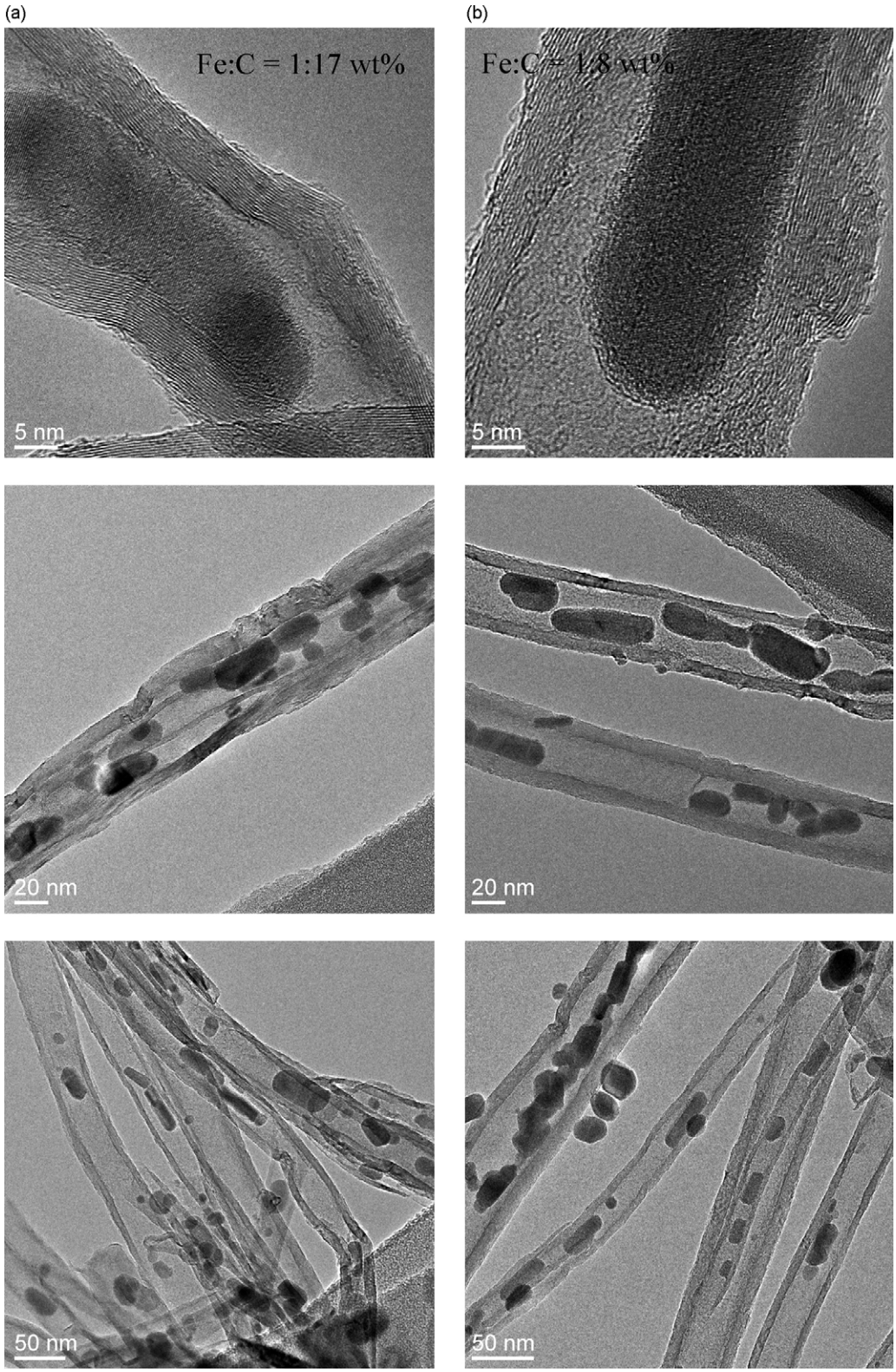

Fig. 2. TEM images of as-prepared Fe_2O_3-filled CNT materials with iron-to-carbon weight ratios of (a) 1:17 and (b) 1:8 at various magnifications.

Fe_2O_3. For particles, Fe_2O_3 is very small (few nanometers) whereas it is much larger (few tens of nanometers) for nanorods. Generally, iron oxide particles are smaller than 50 nm. When Fe:C = 1:17 wt%, almost all of the Fe_2O_3 nanoparticles were inside carbon nanotubes and only a few Fe_2O_3 nanoparticles were distributed outside CNTs. In the case of Fe:C = 1:8 wt%, in addition to Fe_2O_3 nanoparticles inside CNTs, a measurable amount of Fe_2O_3 nanoparticles were present on the surface of CNTs. Fe_2O_3 nanoparticles were smaller with Fe:C = 1:17 wt% than with Fe:C = 1:8 wt%. In both cases, the interior of the

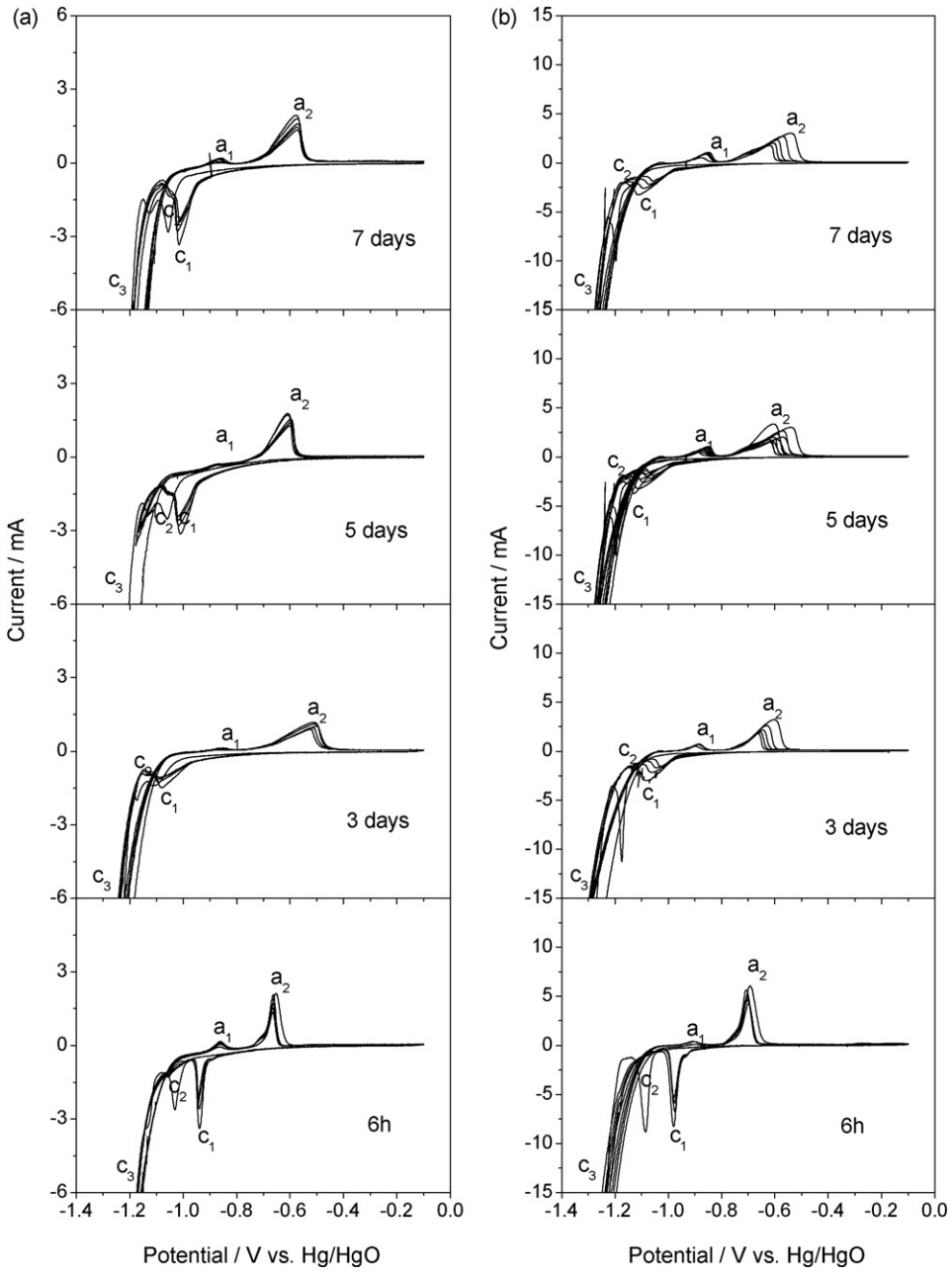

Fig. 3. Voltammograms of Fe_2O_3-filled CNT composite electrodes with (a) Fe:C = 1:17 wt% and (b) Fe:C = 1:8 wt% at various immersion times for electrodes. Scan rate 0.1 mVs^{-1}.

tubes was filled with a large amount of Fe_2O_3 nanoparticles and some spaces remained empty. Such a distribution of Fe_2O_3 is expected to support the redox reaction of Fe_2O_3 and to inhibit an increase in the particle size and dissipation of Fe_2O_3 caused by the re-distribution of iron pieces during cycling via a dissolution–deposition mechanism. The cyclability and capacity of Fe_2O_3-filled CNTs can certainly be improved. However, the penetration of electrolyte into CNTs may be low and this may cause the decrease in electrode capacity.

To determine the effect of penetration of the electrolyte into the CNTs, CV measurements were carried out with various immersion times of electrodes in electrolyte before cycling, and the results are shown in Fig. 3. Several peaks were observed, including a sharp oxidation peak at around −0.65 V (a_2) and a corresponding reduction peak around −0.95 V (c_1), together with a small couple peak at around −0.85 V (a_1) upon oxidation and around −1.05 V (c_2) upon reduction. The anodic peak (a_1) and cathodic peak (c_2) correspond to the Fe/Fe(II) redox couple and peak (a_2) and peak (c_1) correspond to the Fe(II)/Fe(III) redox couple. In the first cycle, the reduction peak c_1 occurred at around −1.04 V, which is a lower potential than in the subsequent cycle, due to the reduction of iron oxide to form iron metal. The peak at around −1.2 V was ascribed to hydrogen evolution (c_3).

The results in Fig. 3 show that the changes in the CV profiles obtained with Fe:C = 1:17 and 1:8 were similar, in that the overpotential increased with an increase in the duration of immersion

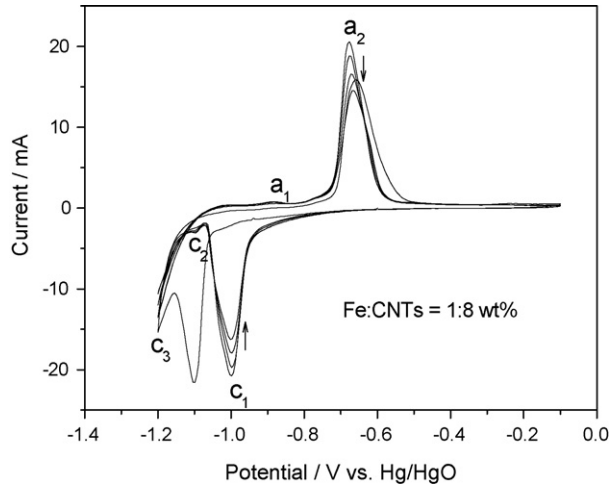

Fig. 4. Voltammograms of Fe_2O_3-loaded CNT composite electrodes with Fe:C = 1:8 wt%. Scan rate 0.1 mVs^{-1}.

of electrodes into electrolyte before cycling, as evidenced by a shifting of oxidation peaks toward more positive and reduction peaks toward more negative. With repeated cycling, the overpotential and redox current decreased and Fe:C = 1:17 wt% showed a smaller decrease than Fe:C = 1:8 wt%. Moreover, Fe:C = 1:17 wt% gave sharp redox peaks while those for FeC = 1:8 wt% were broad. These behaviors support the use of Fe:C = 1:17 wt% during cycling. Thus, the immersion time of an electrode before cycling affected the redox reactions of Fe_2O_3-filled CNTs.

Comparison of these results to CV results for Fe_2O_3-loaded CNTs [27] with Fe:C = 1:8 wt% (Fig. 4) at a sweep rate of 0.1 mVs^{-1} suggested that the two materials, Fe_2O_3-filled CNTs and Fe_2O_3-loaded CNTs, have similar CV profiles. The positions of the redox peaks of both materials are quite similar, however, Fe_2O_3-loaded CNTs showed a greater redox current than Fe_2O_3-filled CNTs. This is reasonable since the redox reaction of Fe_2O_3-loaded CNTs would occur more readily than that of Fe_2O_3-filled CNTs due to the existence of Fe_2O_3 on the CNT surface, which would lead to good contact between Fe_2O_3 and electrolyte. For Fe_2O_3-filled CNTs, the redox reaction may not occur with Fe_2O_3 particles, which reside deep inside CNTs due to the low penetration of electrolyte.

The charge–discharge curves and cycle performance of Fe_2O_3-filled CNTs with Fe:C = 1:17 wt% and Fe:C = 1:8 wt% are shown in Fig. 5. For Fe:C = 1:7 wt%, a plateau occurred at about −0.7 V in discharge and at −0.9 V in charge processes while it appeared at a slightly higher potential in discharge and at a lower potential in charge processes with Fe:C = 1:8 wt%. These plateaus were shifted to a slightly higher potential than with Fe_2O_3-loaded CNTs (Fig. 6). The cycle performance (Fig. 5) showed that in both cases, the changes in the discharge capacity were similar: high capacity at initial cycles and then a gradual decrease. However, Fe:C = 1:17 wt% provided higher capacities than 1:8 wt% after long-term cycling. This can be attributed to the re-distribution of an intermediate soluble species via a dissolution–deposition mechanism. For Fe:C = 1:17 wt%, since almost all of the Fe_2O_3 existed inside CNTs, the re-distribution

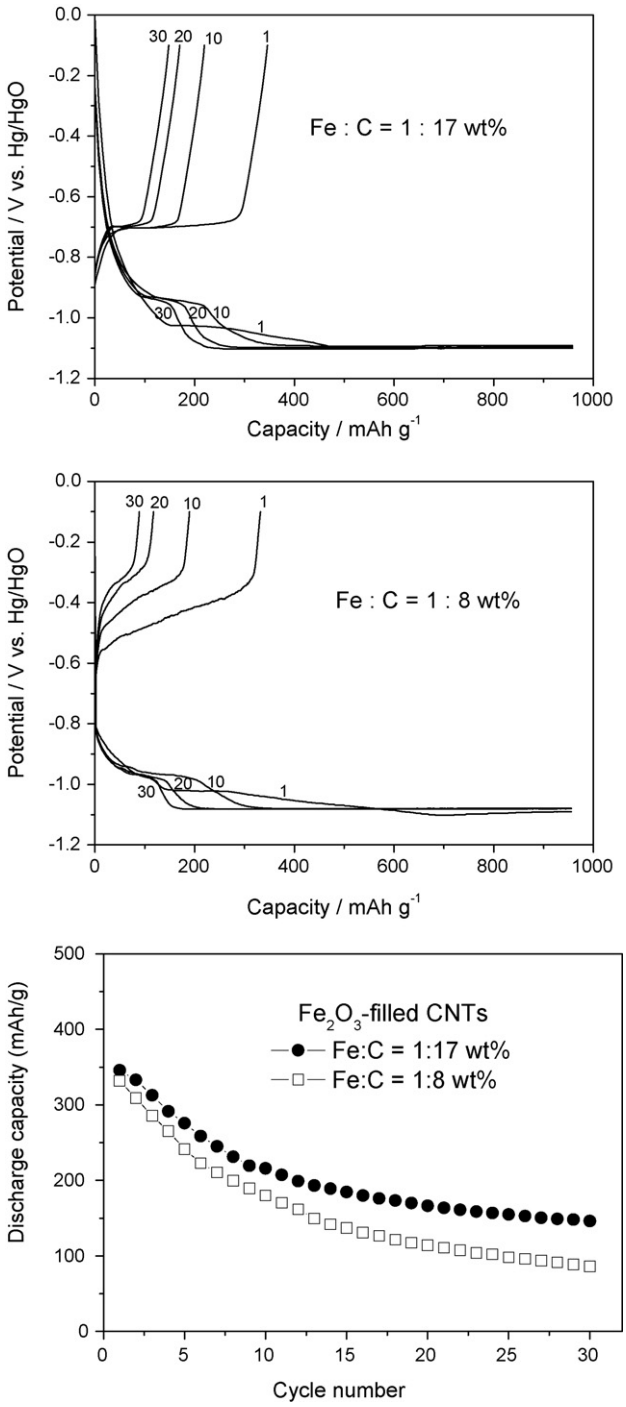

Fig. 5. Charge–discharge curves and cycle performance of Fe_2O_3-filled CNT composite electrodes with Fe:C = 1:17 wt% and 1:8 wt%.

of iron pieces mainly occurred inside CNTs and hence the particle size of iron was limited and the dissipation of soluble species would be reduced. In contrast, for Fe:C = 1:8 wt%, due to the higher iron content and the existence of some Fe_2O_3 particles on the surface of carbon, the size of these particles was not limited and dissipation of soluble species was greater than with 1:17 wt% during cycling, which led to a rapid decrease in capacity. The result in Fig. 5 agrees with the CV profiles in Fig. 3, in which the decrease in redox peaks for Fe:C = 1:17 wt% was smaller than that for 1:8 wt% with repeated cycling.

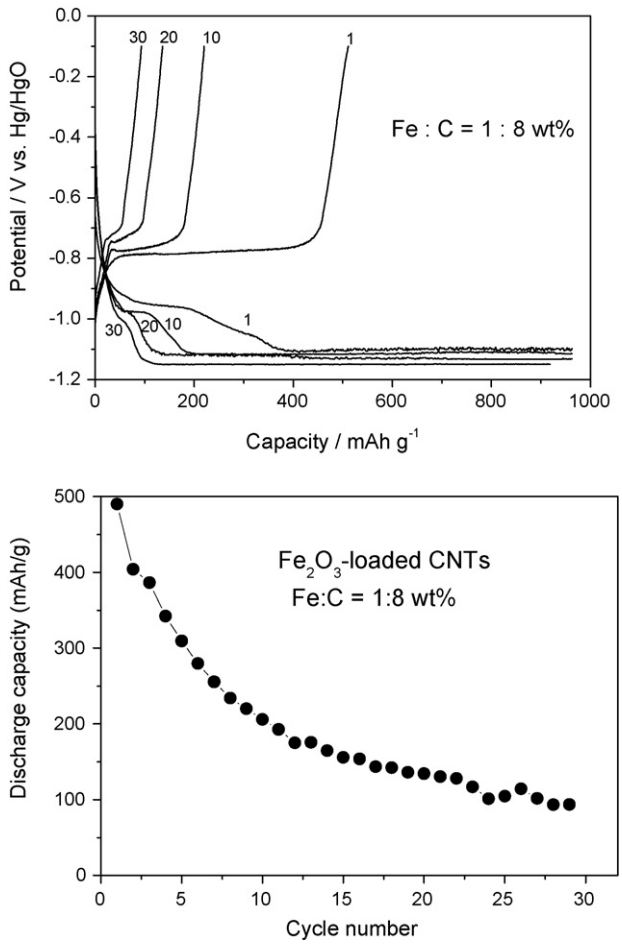

Fig. 6. Charge–discharge curves and cycle performance of nano-sized Fe_2O_3-loaded CNT composite electrode with Fe:C = 1:8 wt%.

The decrease in discharge capacity with repeated cycling may be due to a gradual increase in the passivation of an electrode during cycling. Furthermore, the dissipation of soluble species to the electrolyte also contributed to the fading of capacity.

A comparison of the cycle performance of Fe_2O_3-filled CNTs (Fig. 5) to that of Fe_2O_3-loaded CNTs (Fig. 6) [27] showed that the trends for the changes in capacity were similar. Although Fe_2O_3-loaded CNTs delivered higher capacities than Fe_2O_3-filled CNTs in the initial cycles, Fe_2O_3-filled CNTs provided larger capacity than Fe_2O_3-loaded CNTs with prolonged cycling. For Fe_2O_3-filled CNTs, the penetration of electrolyte inside CNTs is low, which leads to a redox reaction, and this may not occur with some Fe_2O_3 particles, which reside deep inside CNTs. Therefore, in the initial cycles, the capacity of Fe_2O_3-filled CNTs was lower than that of Fe_2O_3-loaded CNTs. Comparison of the results in Figs. 5 and 6 revealed that the cycle performance of Fe_2O_3-filled CNTs was improved in comparison to that of Fe_2O_3-loaded CNTs when Fe:C = 1:17 wt%. This improvement in the capacity of Fe_2O_3-filled CNTs demonstrated that the presence of Fe_2O_3 inside CNTs significantly reduced the dissipation of soluble species during cycling.

To improve the penetration of electrolyte, CNTs were treated by gasification at 300 °C before being used to prepare Fe_2O_3-filled CNTs. With gasification portions of the CNT walls were

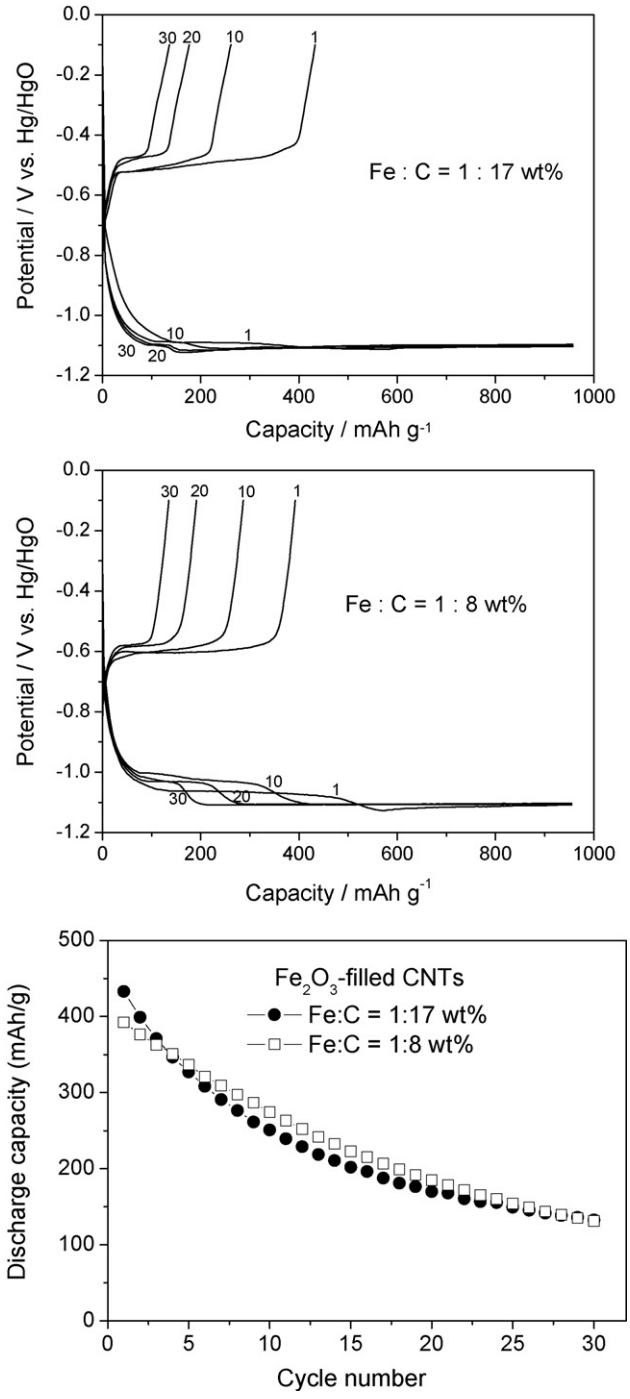

Fig. 7. Charge–discharge curves and cycle performance of Fe_2O_3-filled CNT composite electrodes with Fe:C = 1:17 wt% and 1:8 wt% (CNFs were treated before filling Fe_2O_3).

oxidized and pores were formed. These pores may support the penetration of electrolyte into CNTs, and dissipation may occur. The charge–discharge curves of these samples (Fig. 7) are similar to those of samples using CNTs without treatment (Fig. 5). The cycle performance of Fe_2O_3-filled CNTs using treated CNTs (Fig. 7) showed that a higher capacity could be obtained compared with CNTs without treatment (Fig. 5). However, the capacity still gradually decreased with repeated cycling. This may be caused by the dissipation of soluble species via

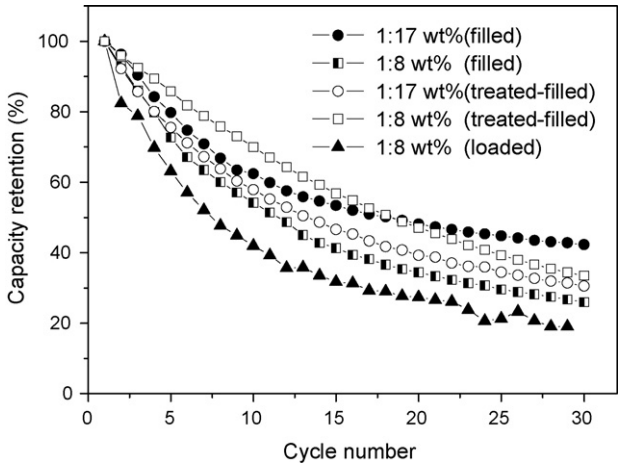

Fig. 8. Capacity retention of Fe_2O_3-filled CNT and Fe_2O_3-loaded CNT composite electrodes.

pores during cycling. Based on a comparison with the cycle performance of Fe_2O_3-loaded CNTs (Fig. 6), the capacity of Fe_2O_3-filled CNTs was significantly improved.

To confirm the advantage of Fe_2O_3-filled CNTs compared to Fe_2O_3-loaded CNTs, the capacity retention was calculated and the results are shown in Fig. 8. It is clear that Fe_2O_3-filled CNTs gave higher capacity retention than Fe_2O_3-loaded CNTs.

It is important to identify the origin of the decrease in capacity with repeated cycling. SEM-EDS measurements were performed on these electrodes before and after the 15th cycle, and the results are presented in Figs. 9 and 10. Before cycling, iron was well-dispersed inside CNTs. Almost no iron was distributed on the carbon surface with both Fe:C = 1:17 wt% and 1:8 wt%. After cycling, iron was distributed on the carbon surface. Larger iron particles were observed outside CNTs after cycling. However, when an electrode containing Fe:C = 1.8 wt% was tested, many large iron particles were observed on carbon, whereas with an electrode containing Fe:C = 1.17 wt%, a very

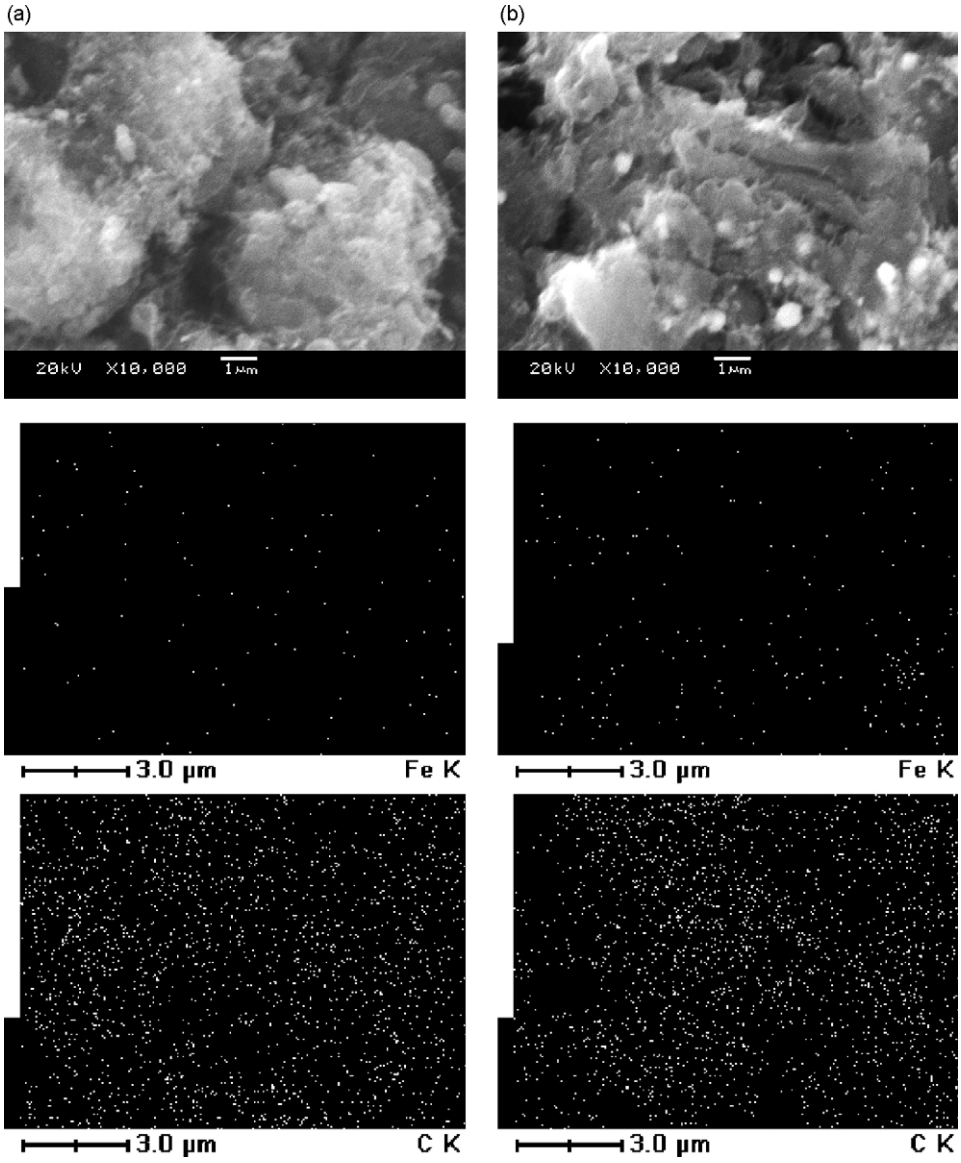

Fig. 9. SEM image and distribution of iron and carbon in electrode containing Fe:C = 1:17 wt% (a) before and (b) after the 15th redox cycle.

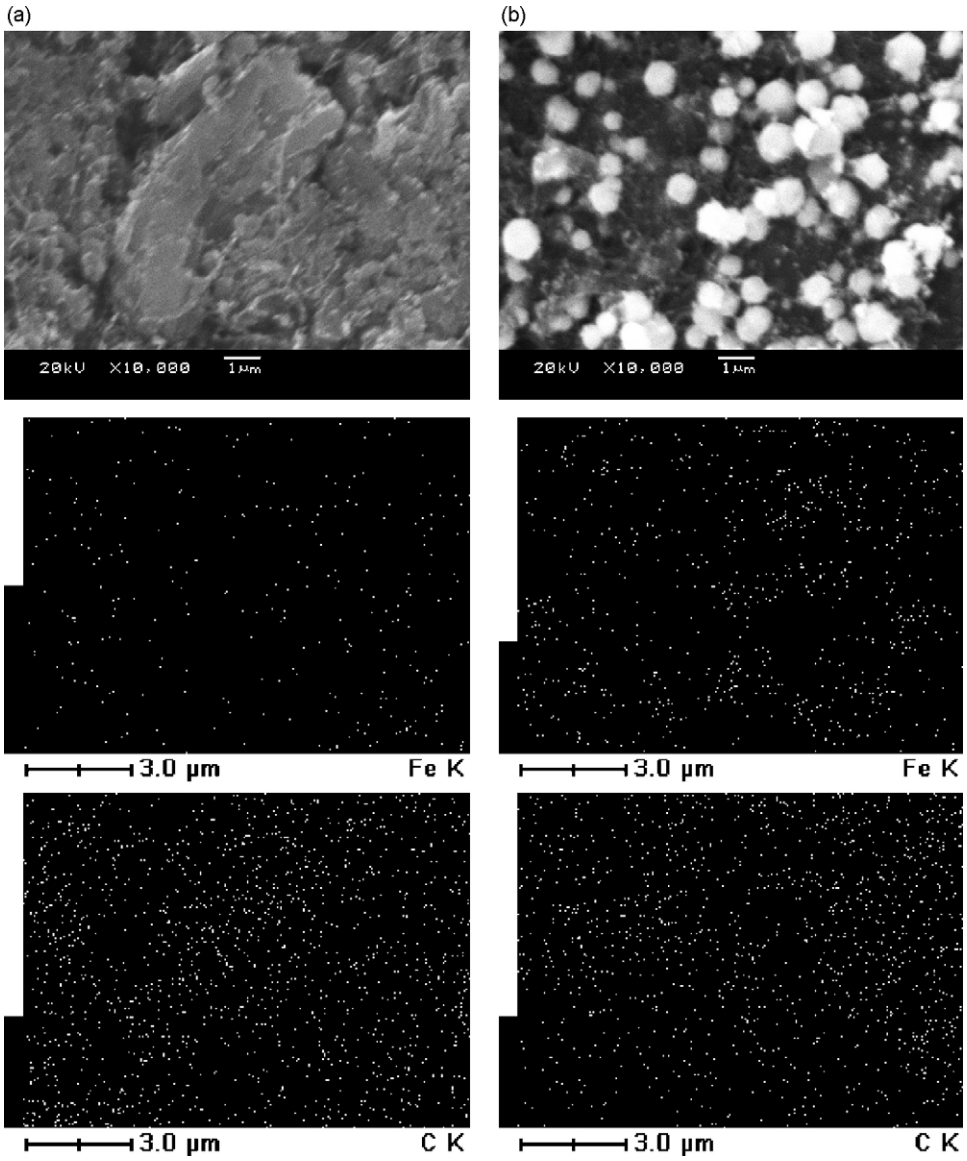

Fig. 10. SEM image and distribution of iron and carbon in electrode containing Fe:C = 1:8 wt% (a) before and (b) after the 15th redox cycle.

small amount of large iron particles were seen on the carbon surface. This is the main cause of the decrease in capacity of each electrode with prolonged cycling. In addition, the dissipation of soluble species upon cycling also contributed to the decrease in capacity. Furthermore, the preparation of electrodes by milling the obtained material with binder probably damaged the material, which led to a decrease in capacity. The SEM–EDS results confirmed the notion that iron was re-distributed by a dissolution–deposition mechanism via an intermediate soluble species $HFeO_2^-$ during cycling. With a further improvement in cycle performance, Fe_2O_3-filled CNTs may be a useful material for the negative electrode of an Fe–air battery.

4. Conclusion

A simple chemical method was used to prepare Fe_2O_3-filled CNT material. The obtained material contains Fe_2O_3 and carbon without any side product. The discharge capacity of Fe_2O_3-filled CNTs was improved compared to that of nano-sized Fe_2O_3-loaded CNTs. Fe_2O_3-filled CNT material is a promising candidate for use in electrochemical devices. Moreover, it may also be useful in various important applications in nanotechnology, biomedical sciences and memory device technology.

Acknowledgement

This work was supported by CREST of JST (Japan Science & Technology Agency).

References

[1] J.I. Pascual, J. Mendez, J. Gomez-Herrero, et al., Science 267 (19951793).
[2] P.G. Collins, A. Zettl, H. Bando, A. Thess, R.E. Smalley, Science 278 (1997) 100.
[3] X.L. Dong, Z.D. Zhang, S.R. Jin, W.M. Sun, X.G. Zhao, Z.J. Li, et al., J. Mater. Res. 14 (19991782).

[4] Z.D. Zhang, J.G. Zheng, I. Skorvanek, et al., J. Phys. Condens. Matter 13 (2001) 1921.
[5] Z.D. Zhang, J.L. Yu, J.G. Zheng, et al., Phys. Rev. B 64 (2001) 4404.
[6] K. Bubke, H. Gnewuch, M. Hempstead, J. Hammer, M.L.H. Green, Appl. Phys. Lett. 71 (1997) 1906.
[7] C. Liu, Y.Y. Fan, M. Liu, H.T. Cong, H.M. Cheng, M.S. Dresselhaus, Science 286 (1999) 1127.
[8] J.A. Misewich, R. Martel, P. Avouris, J.C. Tsang, S. Heinze, J. Tersoff, Science 300 (2003) 783.
[9] A. Bachtold, P. Hadley, T. Nakanishi, C. Dekker, Science 294 (2001)1317.
[10] B. Vigolo, A. Penicaud, C. Coulon, C. Sauder, R. Pailler, C. Journet, et al., Science 290 (2000) 1331.
[11] J. Kong, N.R. Franklin, C.W. Zhou, M.G. Chapline, S. Peng, K.J. Cho, et al., Science 287 (2000) 622.
[12] T.W. Ebbesen, Phys. Today 49 (1996) 26.
[13] I. Monch, A. Meye, A. Leonhardt, K. Kramer, R. Kozhuharova, T. Gemming, et al., J. Magn. Magn. Mater. 290/291 (2005) 276.
[14] F. Okuyama, T. Hayashi, Y. Fujimoto, J. Appl. Phys. 84 (1998) 1626.
[15] S.Y. Chou, M.S. Wei, P.R. Krauss, P.B. Fischer, J. Appl. Phys. 76 (1994) 6673.
[16] J.H.J. Scott, S.A. Majetich, Phys. Rev. B 52 (1995) 12564.
[17] S. Seraphin, D. Zhou, J. Jiao, J. Appl. Phys. 80 (1996) 2097.
[18] S.A. Majetich, J.O. Artman, M.E. McHenry, N.T. Nuhfer, S.W. Staley, Phys. Rev. B 48 (1993) 16845.
[19] W. Weize, Z. Zhenping, L. Zhenyu, X. Yaning, Z. Jing, H. Tiandou, Carbon 41 (2003) 317.
[20] H. Junping, S. Huaihe, C. Xiaohong, Carbon 42 (2004) 3177.
[21] F. Yu, J.N. Wang, Z.N. Sheng, L.F. Su, Carbon 43 (2005) 3018.
[22] L. Suwen, R.J. Wehmschulte, Carbon 43 (2005) 1550.
[23] K. Hansoo, W. Sigmund, Carbon 43 (2005) 1743.
[24] C. Müller, S. Hampel, D. Elefant, K. Biedermann, A. Leonhardt, M. Ritschel, B. Büchner, Carbon 44 (2006) 1746.
[25] H. Junping, S. Huaihe, C. Xiaohong, L. Wentao, Carbon 44 (2006) 2849.
[26] D. Jain, R. Wilhelm, Carbon 45 (2007) 602.
[27] B.T. Hang, T. Watanabe, M. Eashira, S. Okada, J. Yamaki, S. Hata, S. Yoon, I. Mochida, J. Power Sources 150 (2005) 261.
[28] B.T. Hang, M. Egashira, I. Watanabe, S. Okada, J. Yamaki, S. Yoon, I. Mochida, J. Power Sources 143 (2005) 256.